ELSEVIER

Tectonophysics 335 (2001) 313–329

TECTONOPHYSICS

www.elsevier.com/locate/tecto

Magma flow directions of shallow dykes from the East Greenland volcanic margin inferred from magnetic fabric studies

J.-P. Callot[a,1,*], L. Geoffroy[a,2], C. Aubourg[b], J.P. Pozzi[a], D. Mege[c]

[a]*Laboratoire de Géologie, Ecole Normale Supérieure, UMR 8538, 24 rue Lhomond, 75231, Paris, France*
[b]*Département des Sciences de la Terre, Université de Cergy-Pontoise, ESA 7072, 8 Le Campus, 95031 France*
[c]*Laboratoire de Tectonique quantitative, Institut P. and M. Curie, Paris VI, 6 place Jussieu, 75005 Paris, France*

Received 10 July 2000; accepted 21 February 2001

Abstract

The role played by plume-generated crustal magmatic complexes in the segmentation of volcanic margins is highlighted by a preliminary study of magma flow directions in shallow intrusives from the East Greenland volcanic margin. We investigate the magmatic texture using anisotropy of magnetic susceptibility for eight dykes of tholeitic affinity belonging to a dyke swarm associated with the Tertiary opening of the North Atlantic Ocean. The thickness of the sampled dykes ranges from 3 to 37 m. The dykes are of doleritic texture and contain up to 12% of opaque minerals and 35% of plagioclase laths. Dykes showing a magnetic foliation plane within the dyke plane, i.e. a magnetic fabric usually attributed to magmatic processes, represent 40% of the samples from the studied swarm. These dykes have a low degree of anisotropy and their ellipsoid of magnetic susceptibility is strongly oblate. Inverse magnetic fabrics, where the maximum principal susceptibility axis lies near the pole to the dyke account for 60% of the data. We interpret these inverse fabrics either as alteration minerals with highly prolate ellipsoids of magnetic susceptibility or primary titanomagnetites with oblate ellipsoid of low anisotropy. The flow direction is inferred for normal fabric dykes using the mirror imbrication of magnetic lineation. Analysis of thin sections shows a good agreement between magnetic fabric directions and phenocryst preferred orientations. The inferred flow directions are predominantly horizontal, throwing a new light on volcanic margin development.

Keywords: volcanic margin; dyke; basalt; AMS; magnetic fabric; magma flow

1. Introduction

Volcanic margins belong to Large Igneous Provinces which includes continental flood basalts, volcanic margins, oceanic plateaus and ocean basin flood basalts (see a review in Coffin and Eldholm, 1994). Large Igneous Provinces consist of massive emplacements of mafic extrusive and intrusive rocks, emplaced in a short period of time (White and McKenzie, 1989; Richards et al., 1989; Coffin and Eldholm, 1994). Volcanic margins may be related to lithospheric break-up over a mantle plume (Eldholm et al., 1995) when they are clearly associated with abnormally thick adjacent oceanic crust and a hot-spot track and tail.

Volcanic margins differ in several ways from non-volcanic passive margins. Classic volcanic passive margins present the following features: (1) thick

* Corresponding author.
E-mail address: callot@geologie.ens.fr (J.-P. Callot).
[1] Also at: Laboratoire de Géologie, Université du Maine, Faculté des Sciences, avenue O. Messiaen, 72085, Le Mans, cedex 09, France.
[2] Now at: Laboratoire de Géologie, Université du Maine, Faculté des Sciences, avenue O. Messiaen, 72085, Le Mans, cedex 09, France.

0040-1951/01/$ - see front matter
PII: S0040-1951(01)00060-9

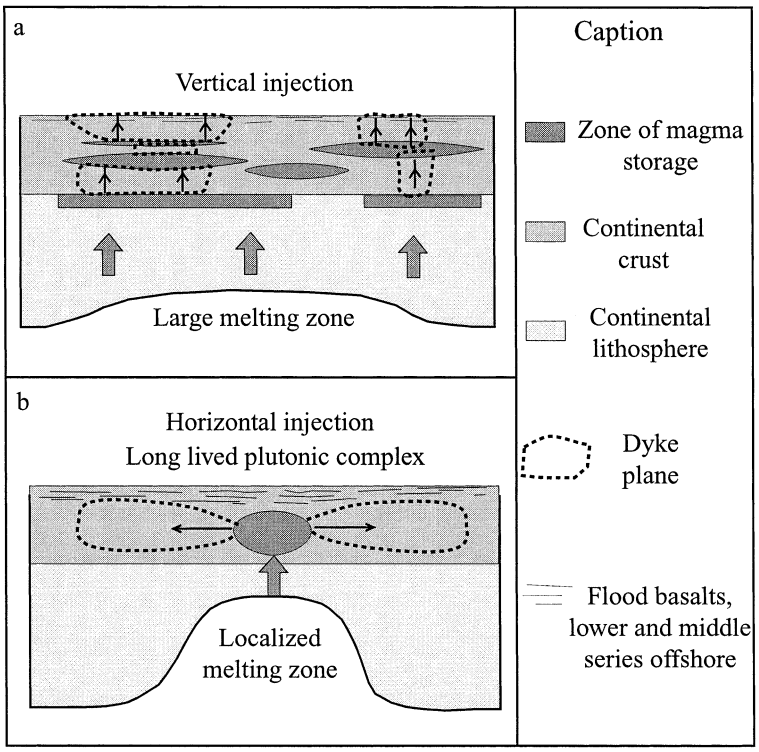

Fig. 1. Schematic sketches illustrating the possible modes of feeding of the extrusive products along a volcanic margin. (a) Vertical injection from sill like magma chambers; (b) horizontal injection from plutonic complexes.

flood basalt sequences onshore continued offshore by thick seaward dipping lava sheets extruded in subaerial conditions (seaward dipping reflectors sequences) (e.g. Hinz, 1981; Eldholm et al., 1995); (2) plutonic complexes associated with dyke swarms parallel to the coast (Myers, 1980); and (3) zones of high seismic velocity in the lower crust likely attributable to magma underplating (White et al., 1987; Eldholm, 1991; Eldholm and Grue, 1994). Despite the numerous studies performed to determine their structures (Mutter, 1984; White, 1992; Eldholm et al., 1995; Geoffroy et al., 2001), the mechanisms by which the extrusive products (flood basalts, SDRS) are fed remains questionable. Along the East Greenland margin, the first magnetic anomaly lies at more than 100 km from the preserved non-intruded continental crust. The transitional continental crust between the first magnetic anomaly and the unaltered continental crust is intruded by the coastal dyke swarm and by numerous intrusive complexes. The dyke swarm, which shows a progressive flexure toward the ocean, may have fed a flood basalt pile tilted oceanward as in the Blosseville promontory. The lava pile was removed by erosion as shown by the estimation of the paleodepth of the actual sea level which is minus 3–4 km (T.F.D. Nielsen, pers. com., 1999). The preserved flood basalts in the northern part of the margin (Bernstein et al., 1998) and the earlier offshore basaltic flows in the southern part of the margin (Saunders et al., 1998) show evidence of crustal contamination and differentiation within continental crust consistent with a model of magma emplacement through the continental crust. On the contrary, the late offshore basaltic series and the SDRS consist of less differentiated and less contaminated basalts and of N-MORB basalts, emplaced through oceanic lithosphere shortly after break-up of the continental lithosphere (Saunders et al., 1998). At volcanic passive margins, the extrusive products, i.e. flood basalts as well as early SDRS, may be fed by

vertical ascent of magma in dykes from the mantle in the case of less differentiated magma (Gudmundsson, 1986, 1990) or from sill like crustal magma storage zones in the case of emplacement through a continental crust (Gudmundsson, 1990) (Fig. 1a). Conversely, the extrusive product may be fed through lateral injection of magma in dykes propagating laterally from plutonic complexes located in the upper crust (Geoffroy, 2000), in a way similar to what have been observed in Iceland at the Krafla volcano (Sigurdsson, 1987), in Hawaii (Knight and Walker, 1988) or in the Azores volcanic system (Moreira et al., 1999) (Fig. 1b). The later model is the most likely as huge plutonic complexes, i.e. long lived volcanic systems, associated to dyke swarms occurred along strike of the East Greenland margin (Fig. 2).

The study of magnetic fabric has proved to be a powerful tool in studying the flow direction in dykes (e.g. Knight and Walker, 1988; Varga et al., 1998; Tauxe et al., 1998). Hence, we conducted a preliminary study of magma flow direction within the East Greenland volcanic margin using anisotropy of magnetic susceptibility (AMS) measurements to constrain the flow direction within the upper crustal dykes and to determine whether the extrusive products are fed by vertical injection of magma from deep sited sill like magma chambers, or by lateral injection from isolated crustal magma chambers.

2. Geodynamical and geological setting

The east coast of Greenland (Fig. 2) provides one of the best exposed volcanic margins (Myers, 1980; Brooks and Nielsen, 1982). Large scale structures on the East Greenland margin appear to be more or less symmetrical with those of the conjugate Norwegian and British margin and may, therefore, provide information that broadly applies to the other volcanic rifted margins of the North Atlantic (Eldholm and Grue, 1994).

The oldest dykes and lavas were erupted as early as 61 Ma, but the most voluminous flood basalts are dated at 57–55 Ma, coeval with continental break-up (Saunders et al., 1998; Tegner et al., 1998). Few major gabbroic plutons, including the Skaergaard gabbros, are associated with the emplacement of the middle lava series onshore during break-up at ~57–55 Ma (Tegner et al., 1998). Most layered gabbro intrusions yield ages around 50–47 Ma (Tegner et al., 1998), younger than the initiation of sea-floor spreading (Fig. 2). North of the Kangerdlussuaq area, the lava pile is largely preserved. The dips of tabular flood basalts systematically increase toward the sea, as an expression of the oceanward flexure of the margin. South of Kangerdlussuaq, 2–3 km of the lava pile has been removed by erosion (Brooks and Nielsen, 1982), and the coast parallel mafic dyke swarms crosscut Precambrian gneisses. The dykes generally trend N–S to N040, and are developed symmetrically apart from igneous centres (Myers, 1980). Here also, the existence of a crustal flexure is attested by the general westward tilt of the main coast-parallel dyke swarm (Myers, 1980; Karson and Brooks, 1999). The dykes display variable dips indicating a syn-flexure emplacement (Karson and Brooks, 1999). A remarkable feature of the margin is the en-échelon pattern of the Tertiary dykes swarms along the margin. Such a pattern suggests an along-strike segmentation of the margin tentatively linked to the activity of localized volcanic complexes (Fig. 2). The gabbros generally give significantly younger $^{40}Ar/^{39}Ar$ ages than the lavas (60 My), ~57–55 Ma for the oldest intrusions and ~50–47 Ma for the more recent (Tegner et al., 1998 and references therein). Some gabbros even locally crosscut lava flows and show similar tilt as the lavas (Myers, 1980). This seems to indicate that the intrusions are located above a localized long-lived fusion zone in the mantle which could be interpreted as mantle diapirs feeding several generations of crustal intrusions. Nevertheless, we cannot exclude a genetic relationship between the extrusive products and associated feeder dykes and the localized melting zone represented by the major gabbroic intrusions. Actually, the $^{40}Ar/^{39}Ar$ ages obtained for the gabbroic intrusions represent cooling ages and, therefore, date the final stage of activity of the plutonic complexes, the activity of which may span over several million years and be significantly older (Tegner et al., 1998; C. Tegner, pers. com., 2000).

For logistic reasons and field conditions, we focused our study of magma flow in dykes in the Erik den Rødes area, where a N080 trending dyke

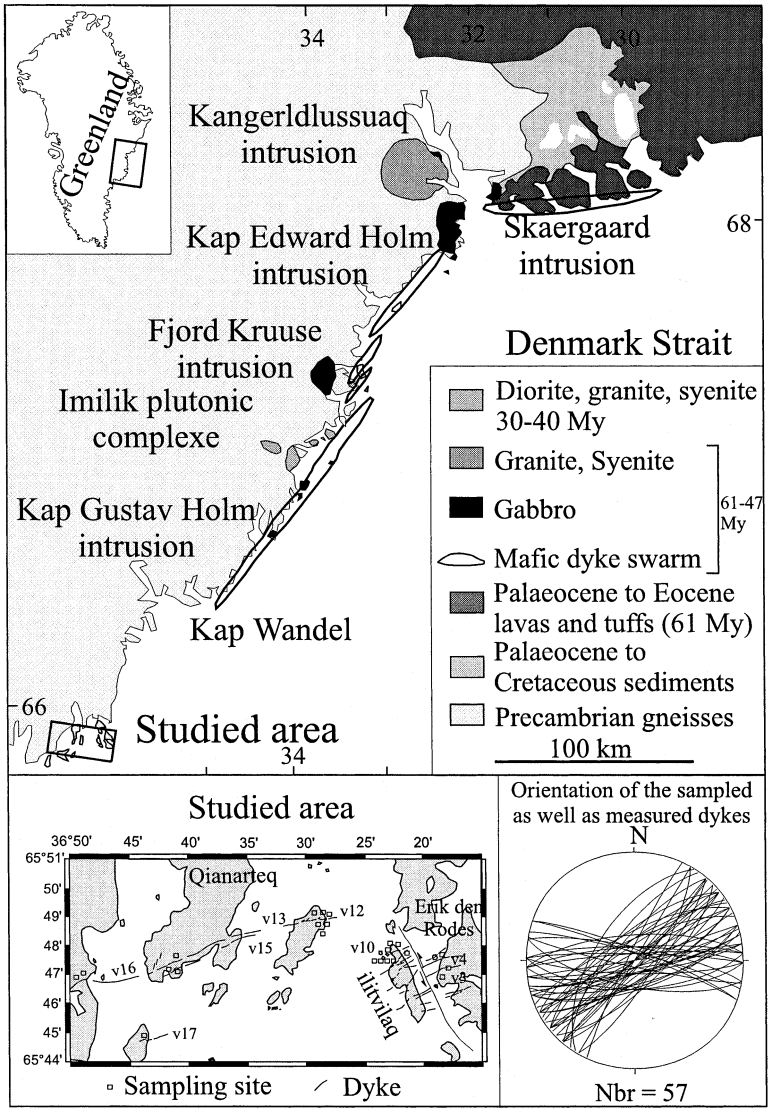

Fig. 2. Geological map of the East Greenland margin, from Myers (1980), with location of the studied area and orientation of the dyke margins. Nbr: number of measured dykes.

swarm outcrops (Fig. 2). These dykes are fresh, unmetamorphosed and exhibit well-preserved thermal jointing, consistent with their assumed Tertiary age. Although they differ in trend from the main Tertiary dyke swarm which outcrops farther north (Myers, 1980), they certainly belong to it and can easily be distinguished from Precambrian dykes which are recrystallized and highly strained under ductile conditions.

3. AMS and magma flow direction

3.1. Background

The anisotropy of magnetic susceptibility (AMS) is generally considered as a reliable tool in studying magma flow in sheeted intrusives (e.g. Knight and Walker, 1988; Ernst and Baragar, 1992; Tauxe et al., 1998; Rochette et al., 1999). AMS is approximated by

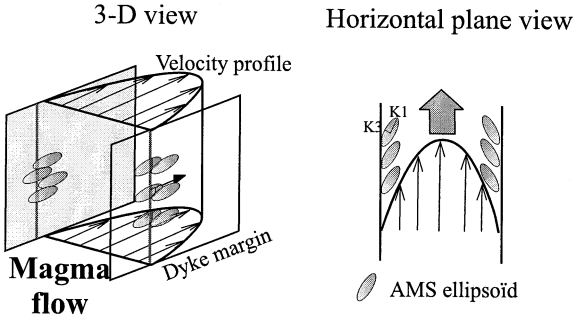

Fig. 3. Relationship between the magnetic ellipsoid and the dyke margin orientation, in case of horizontal flow.

a second rank tensor, and can be described by an ellipsoid with three principal eigenvectors **K1**, **K2** and **K3**, with three eigenvalues $K1 > K2 > K3$. Parameters usually represented are the mean susceptibility $Km = (K1 + K2 + K3)/3$ and the anisotropy ratios L and F (lineation and foliation). In this study, we also used the parameters T and P' to represent the symmetry of shape ($-1 < T < 1$, $T > 0$ for disc shapes and $T < 0$ for rod shapes) and the eccentricity of the ellipsoid, respectively, as defined by Hrouda (1982). In basaltic rocks, AMS is chiefly governed by the ferromagnetic particles, mainly primary titanomagnetites (Hargraves et al., 1991). Several factors can contribute to AMS (review in Rochette et al., 1992, 1999). Among them are (1) orientation of grains, i.e. shape anisotropy (Elwood, 1978), (2) distribution of grains, i.e. distribution anisotropy (Hargraves et al., 1991), and (3) alignment of magnetic domains, i.e. domain anisotropy (Park et al., 1988). It is generally considered that AMS is flow related when the magnetic foliation is closely parallel to the dyke plane, so called 'normal magnetic fabric' (Rochette et al., 1991, 1999; Tauxe et al., 1998). In contrast, the relationship between magnetic lineation and magma flow is questionable, and both parallelism and orthogonality of **K1** with respect to the flow direction were discussed by numerous authors (Khan, 1962; Elwood, 1978; Baer, 1995; Tauxe et al., 1998).

Magnetic lineations have been extensively used previously to infer the sense of flow for several case studies of dykes or sills, with a good agreement with the flow indicators as elongated vesicles or surface lineations (Ernst and Baragar, 1992; Varga et al., 1998). Knight and Walker (1988), following the modelling by Blanchard et al. (1979), first documented for narrow dykes (a few metres thick) an imbrication of magnetic lineation with respect to the dyke margins, which provides a reliable flow direction. Subsequently, several authors used such imbrication of magnetic lineation to infer the flow direction (Staudigel et al., 1992; Varga et al., 1998) (Fig. 3). Tauxe et al. (1998) proposed to infer a unique flow direction when (1) a mirror imbrication exists, (2) fabrics are not highly oblate, and (3) imbrication angles are less than 30°. Tauxe et al. (1998) chose to reject dykes where **K1** clusters differ in inclination by more than 30° ('scissored dyke'). Nevertheless, the mirror geometry of lineation clusters from each margin with respect to the dyke plane is highly dependent on (1) the dyke internal geometry as inclined planar intrusion may not be symmetrical about their mean plane, due to melt and crystal segregation (Komar, 1972; Platten and Watterson, 1987), and also (2) the local departure of the margin, at the scale of an individual core, to the mean trend of the dyke at the scale of the sampling site. We therefore considered as a mirror geometry the existence of bimodal distribution of the magnetic lineation axes, as described by Knight and Walker (1988). In such a case, the cluster of **K1** given by samples from the left-hand-side margins should be offset by 5–30° from the cluster given by the samples from the right-hand-side margin and be offset by a few degrees from the mean dyke plane. We chose to reject scissored dykes following Tauxe et al. (1998).

3.2. Thin section analyses

Direction of flows deduced from magnetic lineations were in some cases successfully compared to structural indicators or to petrofabric axes (Varga et al., 1998). Nevertheless, some authors have pointed out significant discrepancies between magnetic lineation and flow direction (Baer, 1995; Moreira et al., 1999). It thus appears that AMS results must be validated by an independent flow direction estimate. Digital processing of thin sections cut within the foliation plane can, therefore, be performed to measure the angular deviation between the magnetic lineation, i.e. the inferred flow direction, and the preferred orientation of plagioclase phenocrysts, i.e. assumed

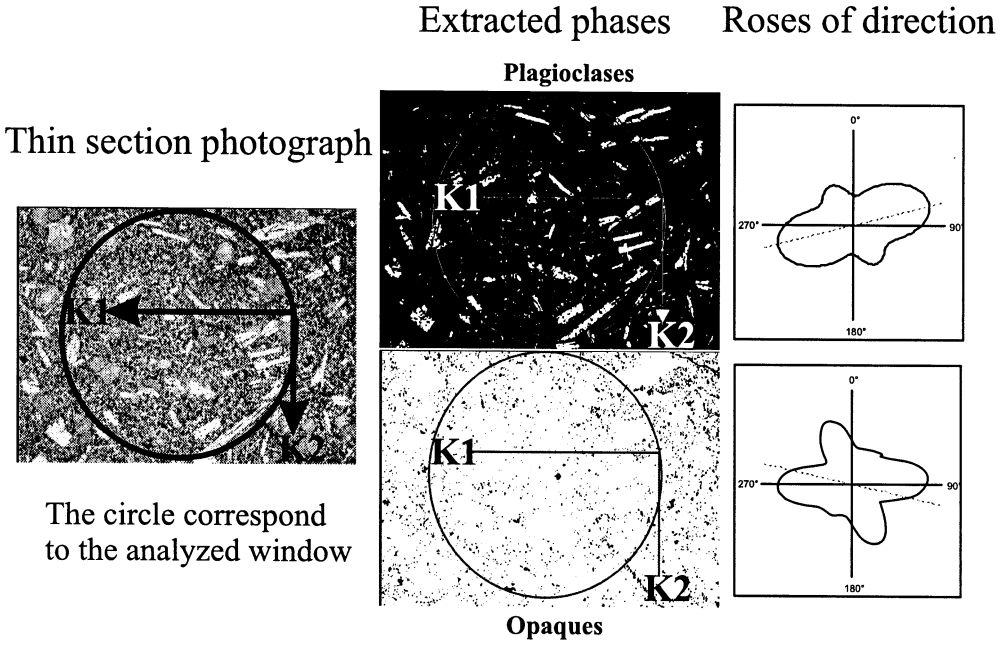

Fig. 4. Thin section analysis method. Example of treatment from a normal fabric dyke, section (JV16, site 25G).

to reflect the real flow direction (Fig. 4). The main errors in our procedure are due to the manual cutting of thin section within the foliation plane. Nevertheless, we estimate them as less than 10° by using a precise orientation device (similar to the core orienting device used in the field). Other errors may follow from the extraction of the minerals' phases from the digitalized photographs but are difficult to estimate. Plagioclase and opaque phases are extracted by processing the original thin section photograph by image filtering. The preferred orientation of a chosen phenocryst phase is estimated using the intercept counting method (Launeau and Robin, 1996). This method analyses the orientation of the boundaries of a chosen phase. Results are displayed as a rose diagram together with the great axes of the calculated mean shape of the phenocrysts. The mean shape may not be meaningful in the case of a non-monomodal fabric, i.e. with two or more different populations of grain with different orientations. We chose to analyse circular windows extracted from the original rectangular photographs to avoid any bias due to the counting method at the boundaries of the photograph.

4. Magnetic studies

4.1. Sampling and measurements

We sampled eight dykes, from 3 to 37 m thick, which were unmetamorphosed and apparently not associated to preexisting fracture sets, an observation suggesting that the dyke injection was not influenced by preexisting features. We chose dykes (1) where both margins were well exposed, and (2) less than a few metres thick when possible to avoid a priori the problem of turbulence (Knight and Walker, 1988; Tauxe et al., 1998). All dykes are of olivine-rich tholeiitic type and contain up to 12% ferromagnetic phases. Unfortunately, macroscopic flow indicators were rare. From 23 to 96 oriented cores were drilled in each dyke, preferentially in the vicinity of the vitrified edges, where the imbrication phenomenon is expected to be more clearly expressed (Knight and Walker, 1988; Tauxe et al., 1998). The dykes were sometimes outcropping over several hundred metres, which allowed us to core a single dyke at different locations (see Table 1). Dyke margins and samples were oriented using both solar and magnetic compass

Table 1
Magnetic and susceptibility results

Dyke	Site	n[a]	Km[b]	L (10^{-3} sd)[c]	F (10^{-3} sd)[d]	P (10^{-3} sd)	T (10^{-3} sd)	$K1$ (D/I)[e]	$K2$ (D/I)	$K3$ (D/I)	$K1$ ($E1$)[f]	$K1$ ($E2$)	$K3$ ($E1$)	$K3$ ($E2$)	Trend[g]	Width (m)
JV3	**17G**[h]	**28**	**57,038**	**1.008(3)**	**1.006(3)**	**1.015(4)**	**−0.129(0.24)**	**63/−7**	**133/72**	**335/17**	**10**	**6**	**8**	**6**	**72S80**	**33**
	18G	**16**	**45,033**	**1.003(1)**	**1.008(2)**	**1.011(2.5)**	**0.474(0.224)**	**66/4**	**301/82**	**336/−6**	**17**	**6**	**9**	**5**	**72S80**	
JV4	19G	26	25,948	1.001(4)	1.004(5)	1.005(7.5)	0.644(0.168)	74/45	332/11	232/43	78	15	39	15	232N75	37
JV10	**9G**	**8**	**43,350**	**1.005(1)**	**1.017(6.5)**	**1.023(7)**	**0.541(0.206)**	**64/18**	**218/70**	**331/8**	**22**	**12**	**16**	**9**	**65S85**	**8**
	10G	11	581,613	1.085(25)	1.008(2.5)	1.104(31)	−0.932(0.066)	339/7	235/62	73/27	5	2	11	4	77S80	
	11G	21	476,748	1.028(15)	1.001(1)	1.034(19)	−0.899(0.168)	331/4	236/47	65/43	5	2	21	4	265N80	
	12G	**9**	**441,887**	**1.002(2)**	**1.006(2.5)**	**1.009(3.5)**	**0.571(0.166)**	**60/3**	**156/59**	**328/31**	**13**	**7**	**7**	**7**	**92S80**	
	13G	**10**	**39,691**	**1.003(0.5)**	**1.008(1)**	**1.011(1.5)**	**0.461(0.088)**	**266/7**	**30/77**	**174/11**	**13**	**5**	**7**	**6**	**77N85**	
	14G	**15**	**413,356**	**1.004(1.5)**	**1.009(2.5)**	**1.013(3)**	**0.413(0.172)**	**256/21**	**47/66**	**162/11**	**17**	**6**	**6**	**4**	**77N85**	
	15G	**12**	**35,840**	**1.004(1.5)**	**1.011(2)**	**1.016(3)**	**0.439(0.122)**	**220/6**	**337/76**	**129/12**	**13**	**7**	**7**	**7**	**220N60**	
	16G	**10**	**39,223**	**1.001(0.5)**	**1.01(2.5)**	**1.013(3.5)**	**0.769(0.114)**	**235/13**	**342/54**	**156/33**	**41**	**14**	**20**	**11**	**220N60**	
JV12–13	1G	5	23,017	1.003(1)	1.003(0.5)	1.006(2.5)	0.062(0.142)	1/7	100/4	195/48	33	22	48	20	92S68	12
	2G	19	34,132	1.003(2.5)	1.003(1)	1.007(3)	−0.004(0.195)	347/5	78/5	214/83	17	6	9	5	67–90	
	3G	14	634,071	1.028(3.5)	1.01(2)	1.039(5)	−0.477(0.79)	354/2	262/40	87/50	9	7	13	8	92–90	
	4G	9	22,240	1.003(1.5)	1.013(1.5)	1.017(3)	0.67(0.106)	27/28	133/28	260/48	26	8	12	5	105N85	
	8G	29	38,843	1.095(23.5)	1.044(8)	1.147(25)	−0.354(0.147)	334/18	210/61	72/23	5	3	6	4	52/90	
JV15	**5G**	**11**	**29,872**	**1.001(1)**	**1.007(3.5)**	**1.008(4)**	**0.374(0.135)**	**100/45**	**276/45**	**8/2**	**56**	**25**	**28**	**24**	**262/90**	**6**
	6G	7	394,186	1.028(10)	1.006(2.5)	1.037(12)	−0.624(0.197)	336/12	98/67	242/12	13	7	66	12	282N85	
	7G	9	41,363	1.05(7.5)	1.034(7.5)	1.087(12)	−0.193(0.129)	348/8	239/67	82/22	5	3	7	4	92N85	
JV16	21G	8	365,692	1.069(14.5)	1.022(4)	1.098(16.5)	−0.503(0.116)	166/11	256/1	352/79	12	10	18	12	230N84	3
	23G	11	30,307	1.073(13)	1.019(8)	1.099(14.5)	−0.574(0.07)	324/3	231/42	58/48	9	3	12	3	50S80	
	24G	12	303,672	1.061(5.8)	1.04(5)	1.103(6)	−0.205(0.07)	119/11	27/13	250/73	18	11	20	10	22N70	
	25G	**16**	**425,138**	**1.006(2)**	**1.017(3.5)**	**1.024(5)**	**0.462(0.109)**	**90/17**	**255/72**	**358/4**	**22**	**7**	**10**	**3**	**105S85**	
	26G	22	240,729	1.014(6.5)	1.014(2.5)	1.028(9)	−0.03(0.118)	161/1	251/9	67/81	18	3	9	2	105S85	
JV17	20G	23	45,904	1.002(1.5)	1.003(2)	1.005(2.5)	0.254(0.178)	300/27	208/4	110/62	54	46	34	26	232N70	9.5

[a] n: number of samples.
[b] Km: mean magnetic susceptibility (10^{-3} SI).
[c] L: lineation parameter with standard deviation.
[d] F: foliation parameter with standard deviation.
[e] D/I: declination and inclination of AMS axes in geographic coordinates.
[f] $E1$–$E2$: 95% confidence angles of AMS axes.
[g] Dyke trend: azimuth, dip to the right direction, dip.
[h] Bold: normal magnetic fabric sites.

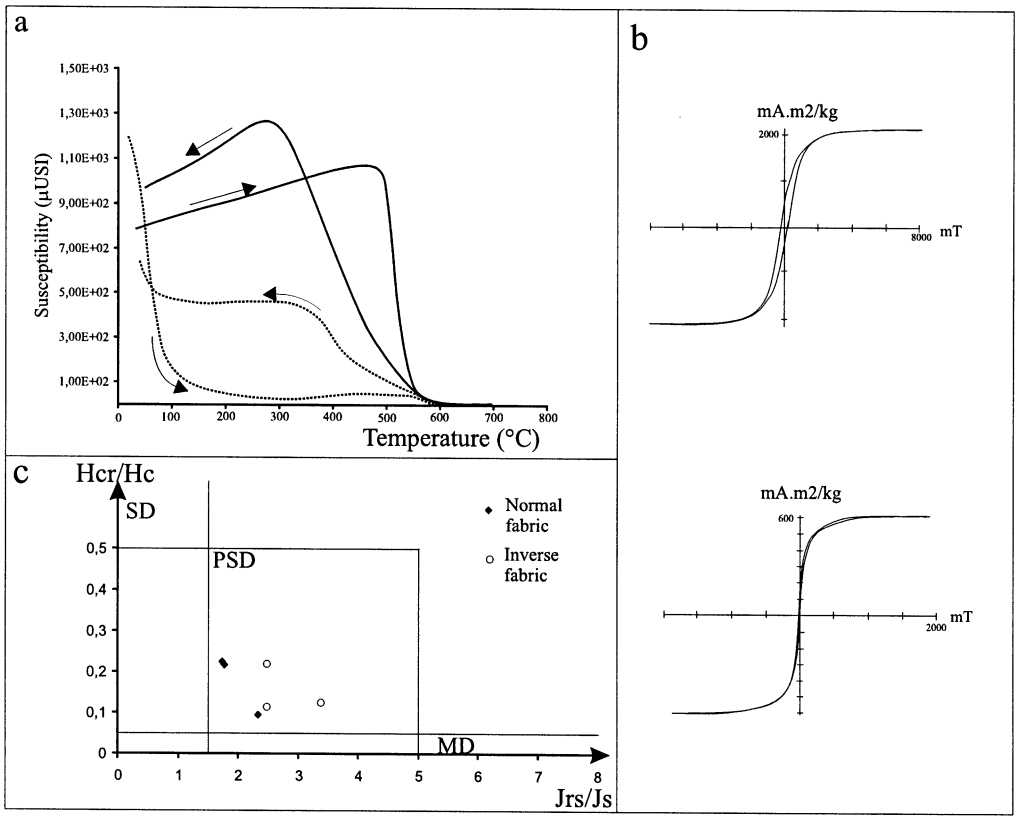

Fig. 5. Rock magnetism results. (a) Susceptibility versus temperature curve; solid line: normal and low anisotropy inverse fabric, example from site 15G; dashed line: high anisotropy inverse fabric, example from site 8G. (b) Typical hysteresis loops, acquired in the St Maur laboratory (IPGP, France; upper cycle: site 15G; lower cycle, site 8G), the lower one showing a wasp-waisted appearance. (c) Day et al. (1977) plot of the hysteresis parameters (sites 15G, 8G, 2G, 7G and 18G).

to avoid magnetic perturbation due to the remanent magnetization of the dyke itself.

However, this sampling strategy displays some possible drawbacks. Due to the vitrified nature of the margin, single-domain magnetite is likely to occur, and can lead to complex permutation of AMS axes (Rochette et al., 1999) as well as secondary recrystallizations and low temperature oxidation (Walderhaug, 1993). By sampling dykes outcropping along the coast, we limit the altering of the rocks due to weathering and bioactivity.

4.2. Rock magnetism

The magnetic susceptibility ranges from 20,000 to 600,000 μSI, indicating a dominant contribution of ferromagnetic grain to AMS results. Curie temperatures were estimated using susceptibility versus temperature curves ($K–T$) measured on a CS3-KLY3S apparatus (Geofyzika, Brno). Measurements were made between room temperature and 700°C, with 2°C temperature steps, a low heating rate and a controlled argon atmosphere to minimize oxidization phenomena. Two different types of $K–T$ curves were observed (end-members are shown in Fig. 5a). In the case of sites with a low degree of anisotropy, which display normal and inverse magnetic fabrics as well (Table 1, Figs. 5 and 6), the $K–T$ curves are close to being reversible and characteristic of a single population of titanomagnetites with low Ti amount (Curie temperatures are well clustered around 540°C). On the contrary, for sites with a high degree of anisotropy (essentially inverse magnetic fabric sites, Table 1, Figs. 5 and 6), $K–T$

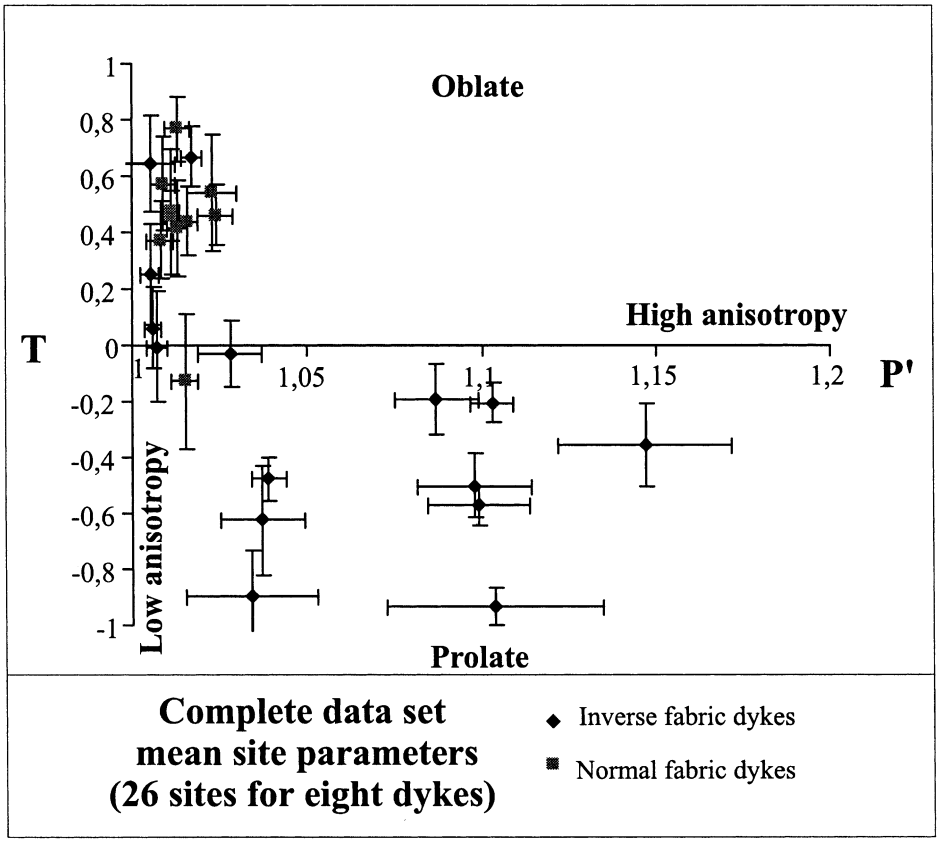

Fig. 6. Shape (T) versus eccentricity (P') parameters. When $T > 0$ (<0) the ellipsoid is oblate (prolate). Uncertainties at the 1/2-σ level.

curves are not reversible. Two Curie temperatures are usually observed, the low temperature one between 100 and 300°C, the high temperature one between 500 and 580°C. Such features are characteristic of a mixture of titanomagnetite with different Ti amount and titanomaghemites. Reversible K–T curves show Curie temperatures ranging from 400 to 570°C, typical of titanomagnetites, with medium to little Ti amount.

Hysteresis loops have been performed at the St Maur laboratory (IPGP, Paris) and confirm the predominance of ferromagnetic titanomagnetites (Fig. 5b). Hysteresis loops typical of PSD grains were obtained for normal magnetic fabric sites (Fig. 5b). Hysteresis parameters for normal magnetic fabric sites ($1.6 < Hcr/Hc < 2.48$; $0.09 < Jrs/Js < 0.23$) also indicate that the titanomagnetites are within the pseudo-single domain state. Hysteresis loops typical of superparamagnetic behaviour but slightly wasp-waisted are sometimes observed for inverse magnetic fabric sites with a high degree of anisotropy (Fig. 5b). A wasp-waisted loop indicates a probable mixture of single domain and superparamagnetic grains (Tauxe et al., 1996).

4.3. AMS results

Magnetic fabrics were measured on a Kappabridge KLY3S apparatus (Geofyzika, Brno), using the 15 positions measurement of Jelinek's procedure (1977). To obtain the mean magnetic anisotropy axes, a tensorial statistic based on linear perturbation analysis is applied (Hext, 1963; Jelinek, 1978). We consider two AMS axes as statistically defined when their 95% confidence ellipses were not overlapping. The use of the linear stability analysis implies that the

Table 2
Mean susceptibility axes for both left-hand-side and right-hand-side margins for normal fabric dykes (except for JV15 for which we have too few samples to calculate representative tensorial means)

	Northern margin						Southern margin					
Dyke	*K*1 (D/I)	*K*3 (D/I)	*K*1–*E*1	*K*1–*E*2	*K*3–*E*1	*K*3–*E*2	*K*1 (D/I)	*K*3 (D/I)	*K*1–*E*1	*K*1–*E*2	*K*3–*E*1	*K*3–*E*2
JV3	68/4	338/6	13	10	15	10	63/7	334/8	10	5	9	5
JV10 (NE–SW trend)	256/21	162/11	17	6	6	4	266/7	174/11	13	5	7	6
JV10 (E–W trend)	224/9	134/0	10	8	17	8	235/13	156/33	41	14	20	11
JV16	282/0	12/4	19	9	12	8	84/27	351/5	31	9	14	4

data have uncertainties that have zero mean, are normally distributed and are small. Such conditions are often reached in homogeneous mafic rocks where AMS is measured using modern equipment, as outlined by Tauxe (1998) for single samples as well as for the entire site. All results are plotted in an equal area projection in the lower hemisphere. Note that the magnetic fabrics are rather well defined with 80% of the confidence angles less than 20° (Table 1). The minimum susceptibility axes **K3** are better defined ($E_{23} = 17.7 \pm 7.3°$) than the maximum susceptibility axes **K1** ($E_{12} = 21.2 \pm 8.9°$) (see Table 1). The magnitudes of the L and F as well as the P' and T parameters are typical of basaltic dykes (e.g. Staudigel et al., 1992; Tauxe et al., 1998), but with a cluster of low values in the oblate ellipsoid field (Fig. 6, Table 1). Dykes showing a magnetic foliation plane subparallel to the dyke plane (so-called 'normal magnetic fabric', Rochette et al., 1991, 1999) constitute roughly 40% of the samples. These have a low degree of anisotropy with an oblate ellipsoid (Fig. 6). On the contrary, inverse magnetic fabric accounts for about 60% of our samples, with a magnetic foliation plane perpendicular to the dyke plane. AMS ellipsoids for inverse fabric range from prolate shaped in case of high degree of anisotropy, to oblate shaped for low degree of anisotropy (Fig. 6, Table 1). It therefore appears that normal magnetic fabric dykes display oblate fabric of low degree of anisotropy, carried by a single population of titanomagnetites. On the contrary, inverse magnetic fabric dykes display either (1) magnetic fabrics and carrier of similar characteristics but with inverse relationship between magnetic axes and dyke geometry, or (2) prolate magnetic fabric of high degree of anisotropy, carried by two or more populations of titanomagnetites and possibly titanomaghemites.

5. Estimation of magma flow

5.1. Inference of flow from AMS results

It is possible to infer a sense of flow from the 'normal fabric dykes' using the classic approach based on the mean **K1** direction and the angular relationship between **K1** and dyke wall (see review in Tauxe et al., 1998). The mean **K1** direction is considered as the flow lineation, the unique flow direction being given by the paired **K1** clusters that represent the imbrication of ferromagnetic grains at the dyke margins (Fig. 3). Four of the eight measured dykes display a normal magnetic fabric. Among them, three show two clusters of **K1** that allow the determination of a unique flow direction (see Table 2). Dyke JV15, which is 6 m thick, shows highly scattered AMS direction. Due to the low number of samples, AMS mean directions are poorly constrained. However, it is possible to infer with high uncertainty a flow lineation, which may be inclined at 40° from the horizontal. The scattering of the data does not preclude that the flow direction may be more horizontal.

The magnetic fabric of dyke JV16 (3 m thickness) is shown in Fig. 7a. As we sampled a segment in which the orientation of the left-hand-side margin differs slightly from the general trend of the dyke at the sampling site, the AMS axes from the left-hand-side margin were rotated as if both margins at the sampling site were parallel. Both **K1** and **K3** axes are rather well grouped. The mean axes of maximum susceptibility are different at a 95% confidence level and illustrate a slight imbrication of about 10° with a mirror geometry with respect to the local trend of the dyke. Nevertheless, those clusters are not symmetrical about the mean dyke plane and the mean axis of maximum susceptibility for the right-hand-side margin has

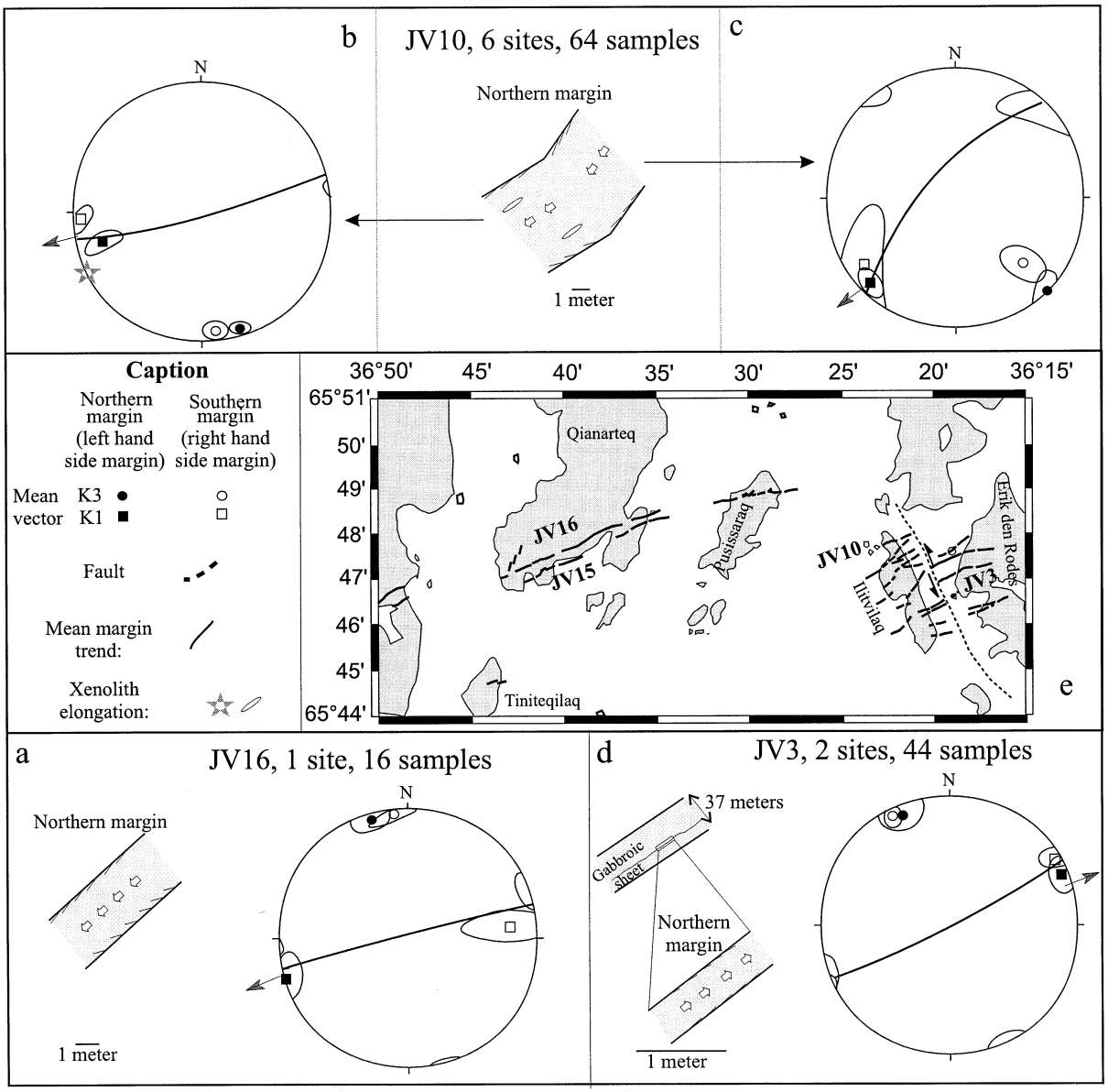

Fig. 7. AMS results for normal fabric dykes with the inferred sense of flow, see text for explanation. a–d: normal fabric dykes, e: reference to the studied zone.

an inclination error greater than 30° and thus should be discarded (Tauxe et al., 1998). According to Knight and Walker (1988) and Tauxe et al. (1998), the flow direction deduced from the imbrication at the left-hand-side margin is subhorizontal and westward directed. This direction is similar to the flow direction deduced from the mirror geometry of the **K1** clusters (Tauxe et al., 1998) and it suggests that the data from the right-hand-side margin are relevant to the flow direction.

Fig. 7b and c are the plots for the dyke JV10. This dyke is on average 8 m thick. It was sampled at different height locations up to a few hundred metres apart, six of which display normal magnetic fabrics, thus

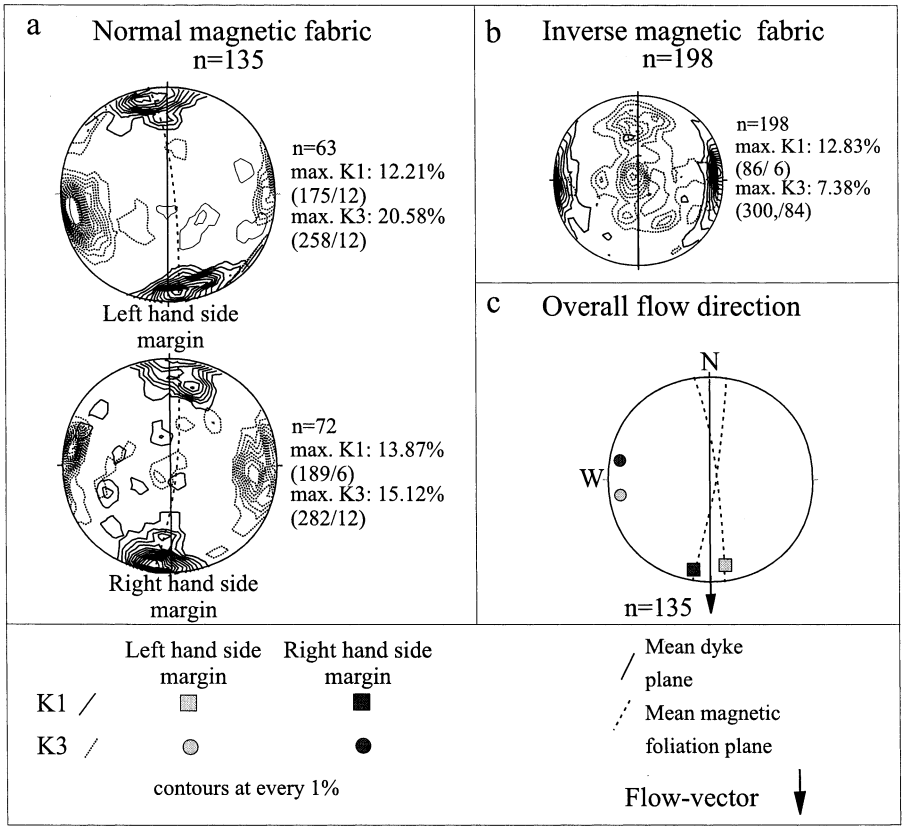

Fig. 8. (a) Normal magnetic and (b) inverse magnetic fabric dykes plotted in dyke coordinates. The dyke planes are vertical, with a N–S trend, after rotation. (c) Determination of average flow vector for the entire data set from normal fabric dykes.

related to magmatic flow. Two major azimuths for the dyke were recognized in the field, and two pairs of clusters of magnetic axes, therefore, arise on the stereoplot, each of them showing an imbrication geometry (Tauxe et al., 1998). Here again, it is difficult to attest that the **K1** clusters are symmetrical about the dyke plane as the local margin orientations differ in some places from the mean dyke azimuth. Thus, the mirror geometry is not achieved here in the meaning of Tauxe et al. (1998), but there is a clear imbrication of magnetic lineation as described by Knight and Walker (1988), which allows us to infer an absolute sense of flow. The magnetic lineation clusters are well grouped and offset by 11° in the case of the E–W trending sites (Fig. 7b). The clusters are not different at a 95% confidence level for the NE–SW trending sites, but they display a similar imbrication with an offset of less than 10°. Both clusters are compatible with a horizontal WSW directed magma flow, with little plunge downward. This sense of flow is consistent with the orientation of elongated gneiss xenoliths measured in the field. Note that we obtain the same sense of flow for six of the eight sampling locations which are dispatched along a 3 km long outcrop of the dyke, the two others being inverse magnetic fabric sites.

Fig. 7d is the plot for dyke JV3. The samples were taken in a 50 cm thickness gabbroic sheet within a 37 m thickness dyke. The gabbroic sheet is situated 7 m away from the eastern margin. The mean magnetic lineation is rather well constrained and indicates a subhorizontal flow lineation. On the contrary, the minimum susceptibility axes are scattered within a plane perpendicular to the dyke. The average susceptibility ellipsoid is rather triaxial, as the magnetic foliation poles are scattered within a plane perpendicular

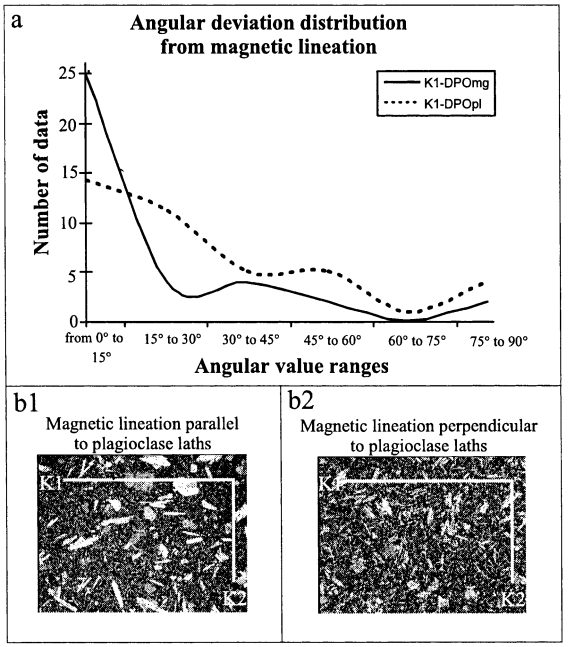

Fig. 9. Thin section study. (a) Angular deviation between the measured magnetic lineation and the preferred orientation of (1) opaque minerals (*K*1-DPOmg, solid line) and (2) plagioclase phenocrysts (*K*1-DPOpl, dashed line). (b) Example of parallelism between magnetic lineation and plagioclase laths (b1, dyke JV16, site 25G) and of orthogonality (b2, dyke JV10, site 15G).

to the dyke plane. Nevertheless, the ellipsoid is oblate at the scale of a plug. The mean magnetic lineation from each margin is not different at the 95% confidence level. Although they seem to draw an imbrication with respect to the dyke margins which may allow us to infer an absolute sense of flow, the apparent sense of flow may be an artefact due to the poor definition of the **K1** clusters. We thus may only infer from this dyke the flow lineation, which is horizontal.

5.2. Overall flow direction

If one plots the AMS axes for all the dykes which bear a normal magnetic fabric in dyke coordinates (i.e. the dykes being rotated to a N–S strike and tilted to the vertical, Rochette et al., 1991) (Fig. 8a), the magnetic axes appear remarkably well clustered. The **K1** and **K3** clusters display the perfect mirror geometry which is necessary to infer both direction and sense of flow (Tauxe et al., 1998). In the case of the sites with inverse magnetic fabric, the magnetic lineations are well clustered perpendicular to the dyke plane, but show no mirror geometry (Fig. 8b). The minimum susceptibility axes show a poorly defined vertical maximum. From the normal fabric dykes data set, it is possible to infer an average flow direction. The magnetic lineations are well grouped statistically at each margin of the dykes and they define an imbrication from which we can deduce the absolute sense of flow. The two clusters of **K1** are offset from the rotated dyke walls by 9 and 5°, respectively, and are mainly within 25° from the horizontal. This average sense of flow is horizontal and it is systematically directed southward in dyke coordinates (Fig. 8c). The flow direction is generally southwestward directed in geographic reference.

5.3. Thin sections analyses

Twenty oriented thin sections were cut within the magnetic foliation plane, i.e. plane (**K1**, **K2**) of samples from normal magnetic fabric dykes. We took 40 representative pictures which were analysed. A rather good agreement between the magnetic lineation direction and the preferred orientation of plagioclases is observed (Fig. 9a). In most cases (66%), the magnetic lineation is within less than 30° from the preferred orientation of plagioclases laths (Fig. 9b). The magnetic lineations which are perpendicular to the plagioclases laths (Fig. 9c) may be a consequence of a 'rolling effect', as described by Jeffery (1922). Despite this discrepancy, the good agreement suggests that the plagioclase petrofabric is flow related. Moreover, a very good agreement between opaque preferred orientation and magnetic lineation is obtained, suggesting that the AMS signal is due either to a shape anisotropy of ferromagnetic grains or to an anisotropy of distribution of ferromagnetic grains mimicking the plagioclases' flow related fabric, as pointed out by Hargraves et al. (1991). The AMS signal is, therefore, likely to reflect the flow related petrofabric in the case of normal magnetic fabric dykes.

6. Discussion

Our four normal fabric dykes show a rather well constrained horizontal cluster of magnetic lineation,

suggesting a more or less horizontal flow direction. Two of them, JV16 and JV10, display imbrication of magnetic lineation consistent with a southwestward to westward directed flow and consistent with the average flow direction, which is estimated on the basis of the entire data set (Figs. 7 and 8). Dyke JV3 is a 37 m thick dyke showing heterogeneous grain size. It presents, particularly at 7 m from the southern margin, a thin gabbroic sheet of variable thickness, but separated from the other part of the dyke by a 'hot' contact between magmas of different grain sizes. We sampled this sheet at two locations where it was ~50 cm thick. We observed a good clustering of AMS axes and an apparent offset of the **K1** cluster of each margin by 5° from the other. However, the 95% confidence ellipse for the **K1** axes are overlapping and this does not allow one cluster to be distinguished from the other. From the AMS result, we can infer a horizontal flow lineation for dyke JV3. Nevertheless, from the apparent imbrication of the **K1** axes, we may infer that the sense of flow is northeastward directed. On the contrary, the general flow direction and the flow direction of dykes JV10 and JV16 are southwestward directed. This result may arise from poorly constrained AMS axes and imbrication, but could tentatively be linked to magmatic processes. This apparent discrepancy may be a consequence of a backflow (Philpots and Asher, 1994), as the porphyritic gabbro may have crystallized late in the dyke history and it may have been subjected to the late evolution of the feeding magmatic chamber. Moreover, such thick dykes are likely to be fed by several pulses of magma (Platten and Watterson, 1987) flowing within solidified anterior magma already accreted to the margin. However, as we do not observe well defined comb layers due to crystallization of the inner sheet on a solid substrate (Platten and Watterson, 1987), the inner gabbroic sheet was probably emplaced and crystallized within fluid less porphyritic magmas. A velocity contrast between the gabbroic sheet and surrounding magma should arise from the grain size difference as the viscosity of a magma is highly dependent on its solid fraction (Nicolas, 1992). The higher the solid fraction, the higher the viscosity. Thus, an apparent northeastward directed flow direction can arise if the inner gabbroic sheet velocity is lower than the velocity of the surrounding magma, as a consequence of the higher viscosity of the gabbros.

The 8 m thick dyke JV10 outcrops over about 3 km. The dyke presents also two different azimuths in the field. These features allowed us to core the dyke at eight different localities and test the reliability of the flow direction inferred from measurements of anisotropy of magnetic susceptibility. Fortunately, six of the sampling sites display normal magnetic fabric. In order to infer a flow direction, we pooled the data from the sampling sites which display the same azimuth. It is interesting that the two sub-datasets obtained both display an imbrication geometry of magnetic lineation. The mean magnetic lineations from the data set which have an east–west trend are different at a 95% confidence level and, thus, defined a flow direction, toward the east-south-east (Fig. 8b). The result is close to the expected mirror geometry (Tauxe et al., 1998). The magnetic lineations from the other sub-dataset are not different at a 95% confidence level and, thus, we cannot determine the flow direction, rather a flow lineation which is horizontal, although the imbrication of the two mean **K1** axes may reflect the same flow direction (Fig. 8c). AMS inferred flow directions are consistent from the scale of a plug (one inch) to the scale of a dyke (several hundred metres). The consistency of the data ranges over five orders of scale magnitude. This result is not obvious as magma flow is strongly controlled by local centimetre scale heterogeneities of the margin (Platten and Watterson, 1987). Our results also emphasize the importance of the imbrication geometry in obtaining reliable flow direction. Lineation of flow is given by the direction of the mean maximum principal susceptibility axis, which when considered alone does not offer any indication on the sense of flow (for example in the case of dyke JV15). On the contrary, the imbrication geometry gives the direction of flow. The mirror geometry as described by Tauxe et al. (1998) corresponds to a particular case of perfectly symmetrical planar dyke. As dykes often show mineral as well as grain size segregation linked to flow differentiation (Komar, 1972), particularly in the case of primary non-vertical intrusions, a perfect symmetry of magnetic axes about the dyke plane may be rather uncommon. Actually, we observe a rather bimodal distribution of **K1** axes, the clusters associated to the margins being offset by 6–15°. Following Knight and Walker (1988), we consider such imbrication as a reliable flow indicator.

Note that the imbrication with respect to a single margin—i.e. the tiling of the lineation along the margin—can be deceiving as shown in Fig. 8. In most cases, the magnetic lineation is sub-parallel to the margin, a scheme that does not allow a sense of flow to be inferred, or it draws an imbrication geometry which gives a sense of flow opposite to the real sense of flow. It is essential to core both margins of the dyke to obtain the real flow related imbrication of magnetic lineation and distinguish (1) a flow related but nonsymmetric with respect to dyke plane imbrication of **K1** from (2) a scissored distribution of **K1** typical of sheared dykes which draws no imbrication of **K1** clusters (Rochette et al., 1991; Tauxe et al., 1998).

7. Conclusions

This preliminary study focused on 361 samples from eight dykes from a coastal dyke swarm of East Greenland. Inferring the sense of magma flow using AMS lineation, we find that the flow-vectors are predominantly horizontal to slightly downward (Fig. 8). Although based on a relatively small number of dykes (but an important number of samples), our results are consistent from the scale of a plug to the scale of a dyke, over five orders of magnitude of scale. Our results suggest the existence of a localized magma source which may have been situated at a shallow level in the brittle crust, as the paleodepth estimate is about 3–4 km (T.F.D. Nielsen, pers. com., 1999). The extrusive products were probably fed by dykes propagating laterally from magma chambers located in the upper crust. The study of the coastal dyke swarm of East Greenland showed magmatic dilatation gradient increasing toward coastal igneous centres (Myers, 1980). Lateral injection of dykes from crustal magma chambers have already been documented by the means of seismic recording in Iceland, as well as through AMS measurements in Skye Island (Sigurdsson, 1987; Geoffroy and Aubourg, 1997). Our results suggest a similar mode of dyke injection from high level magma chamber at volcanic passive margins, tentatively linked to the coastal gabbro and syenite complexes outcropping along the east coast of Greenland. Volcanic passive margins are possibly fed by localized independent accretion centres. Similar focused magmatic accretion arose from the study of volcanic complexes—e.g. an active one in Iceland (Gudmundsson, 1990) or extinct ones from the British Tertiary Igneous Province (Speight et al., 1982)—as well as from both active and extinct spreading ridges—Oman (Staudigel et al., 1992) and Mid Atlantic ridge (Lin et al., 1990). Thus our results suggest similar mechanisms of melt production and segregation in these different geodynamical settings.

Acknowledgements

R. Ernst and J.S. Gee are gratefully acknowledged for their remarks and criticisms which contributed to improve an early draft of the manuscript. The field work was supported by the French Polar Institute (IFRTP) and the Institut National des Sciences de l'Univers (CNRS-INSU). The 1998 field party was composed of L. Geoffroy, C. Aubourg and D. Mege.

References

Baer, G., 1995. Fracture propagation and magma flow in segmented dykes: field evidences and fabric analyses, Makhtesh Ramon, Israel. In: Baer, G., Heimann, A. (Eds.), Physics and Chemistry of Dykes. Balkerna, Rotterdam, pp. 125–140.

Bernstein, S., Kelemen, P.B., Tegner, C., Kurz, M.D., Blusztajn, J., Brooks, C.K., 1998. Post-breakup magmatism along the East Greenland Tertiary rifted margin. Earth Planet. Sci. Let. 160, 845–862.

Blanchard, J.-P., Boyer, P., Gagny, C., 1979. Un nouveau critère de mise en place dans une caisse filonienne: le 'pincement' des minéraux aux épontes. Tectonophysics 53, 1–25.

Brooks, C.K., Nielsen, T.F.D., 1982. The E. Greenland continental margin: a transition between oceanic and continental magmatism. J. Geol. Soc. London 136, 265–275.

Coffin, M.F., Eldholm, O., 1994. Large igneous provinces: crustal structure, dimensions and external consequences. Rev. Geophys. 32, 1–36.

Day, R., Fuller, M.D., Schmidt, V.A., 1977. Hysteresis properties of titanomagnetites: grain size and composition dependence. Phys. Earth Planet. Int. 13, 260–266.

Eldholm, O., 1991. Magmatic evolution of a volcanic rifted margin. Mar. Petrol. Geol. 102, 43–61.

Eldholm, O., Grue, K., 1994. North Atlantic volcanic margins: dimensions and production rates. J. Geophys. Res. 99, 2955–2968.

Eldholm, O., Skogseid, J., Planke, S., Gladczenko, T.P., 1995. Volcanic margins concepts. In: Banda, E. et al. (Eds.), Rifted

Continent Ocean Boundaries, NATO ASI Series. Kluwer Academic Publishers, Dordrecht, pp. 1–16.

Elwood, B.B., 1978. Flow and emplacement direction determined for selected basaltic bodies using magnetic susceptibility anisotropy measurements. Earth Planet. Sci. Let. 41, 254–264.

Ernst, R.E., Baragar, W.R.A., 1992. Evidence from magnetic fabric for the flow pattern of magma in the MacKenzie giant radiating dyke swarm. Nature 356, 511–513.

Geoffroy, L., 2000. The structure of volcanic margins: some problematics from the North-Atlantic/Labrador-Baffin system. Mar. Petrol. Geol. (in press).

Geoffroy, L., Aubourg, C., 1997. Magma injection around plume-related high-level ultramafic bodies in Skye Island: a study with AMS. Terra Nova Abstract.

Geoffroy, L., Callot, J.P., Skuce, A.G., Scaillet, S., Gélard, J.P., Ravilly, M., Angelier, J., Cayet-Cauvin, C., Bonin, B., Lepvrier, C., 2001. The South-Baffin Bay volcanic margin: NAM–Greenland plate separation over a mantle plume. Tectonics (in press).

Gudmundsson, A., 1986. Mechanical aspects of post-glacial volcanism and tectonics of the Reykjanes Peninsula. J. Geophys. Res. 91, 12711–12721.

Gudmundsson, A., 1990. Emplacement of dykes, sills and crustal magma chambers at divergent plate boundaries. Tectonophysics 176, 257–275.

Hargraves, R.B., Johnson, D., Chan, C.Y., 1991. Distribution anisotropy: the cause of AMS in igneous rocks? Geophys. Res. Let. 18, 2193–2196.

Hext, G., 1963. The estimation of second-order tensor, with related tests and designs. Biometrika 50, 353–357.

Hinz, K., 1981. Hypothesis on terrestrial catastrophes: wedges of very thick oceanward dipping layers beneath passive margins—their origins and palaeoenvironment significance. Geol. Jahrb. 22, 345–363.

Hrouda, F., 1982. Magnetic anisotropy and its application in geology and geophysics. Geophysical Surveys 5, 37–82.

Jeffery, G.B., 1922. The motion of ellipsoidal particles immersed in a viscous fluid. Proc. R. Soc. London 102, 161–179.

Jelinek, W., 1977. The statistical theory of measuring anisotropy on groups of specimens and its application. Geofyzyca, Brno.

Jelinek, V., 1978. Statistical processing of anisotropy of magnetic susceptibility measured on groups of specimens. Stud. Geophys. Geod. 22, 50–62.

Karson, J.A., Brooks, C.K., 1999. Structural and magmatic segmentation of the Tertiary East Greenland volcanic rifted margin. In: Ryan, P., McNiocaill, C. (Eds.), J.F. Dewey Volume on Continental Tectonics. Geol. Soc. Spec. Publ. 164, pp. 313–318.

Khan, M.A., 1962. Anisotropy of magnetic susceptibility in some igneous and metamorphic rocks. J. Geophys. Res. 67, 2873–2885.

Knight, M.D., Walker, G.P.L., 1988. Magma flow direction in dykes of the Koolau complex, Oahu, determined from magnetic fabric studies. J. Geophys. Res. 93, 4301–4319.

Komar, P.D., 1972. Flow differentiation in igneous dykes and sills: profiles of velocity and phenocrysts concentration. Geol. Soc. Am. Bull. 83, 3443–3448.

Launeau, P., Robin, P.-Y.F., 1996. Fabric analyses using the intercept method. Tectonophysics 267, 91–119.

Lin, J., Purdy, G.M., Schouten, H., Sempere, J.C., Zervas, C., 1990. Evidence from gravity data for focused magnetic accretion along the Mid-Atlantic Ridge. Nature 334, 627–632.

Moreira, M., Geoffroy, L., Pozzi, J.-P., 1999. Ecoulement magmatique dans les dykes du point chaud des Açores: etude préliminaire par anisotropie de susceptibilité magnétique ASM dans l'Île de San Jorge. C.R. Acad. Sci. Paris 329, 15–22.

Mutter, J.C., 1984. Seaward dipping reflectors and the continent ocean boundary at passive continental margins. Tectonophysics 114, 117–131.

Myers, J.S., 1980. Structure of the coastal dyke swarm and associated plutonic intrusion of east-Greenland. Earth Planet. Sci. Let. 46, 407–418.

Nicolas, A., 1992. Kinematics in magmatic rocks with special reference to gabbros. J. Petrol. 33, 891–915.

Park, J.K., Tanczyk, E., Debarats, A., 1988. Magnetic fabric and its significance in the 1400 Ma Mealy diabase dykes of Labrador, Canada. J. Geophys. Res. 93, 13689–13704.

Philpotts, A.R., Asher, P.M., 1994. Magmatic flow-direction indicators in a giant diabase feeder dike, Connecticutt. Geology 22, 363–366.

Platten, I.M., Watterson, J., 1987. Magma flow and crystallization in dike fissures. In: Halls, H.C., Fahrig, W.F. (Eds.), Mafic Dyke Swarms. Geol. As. Can. Spec. Pap. 34, pp. 65–73.

Richards, M.A., Duncan, R.A., Courtillot, V., 1989. Flood basalts and hot-spot tracks: plume heads and tails. Science 246, 103–107.

Rochette, P., Aubourg, C., Perrin, M., 1999. Is this magnetic fabric normal? A review and case studies in volcanic formations. Tectonophysics 307, 219–234.

Rochette, P., Jackson, M., Aubourg, C., 1992. Rock magnetism and the interpretation of anisotropy of magnetic susceptibility. Rev. Geophys. 30, 209–226.

Rochette, P., Jenatton, L., Dupuy, C., Boudier, F., Reuber, I., 1991. Emplacement modes of basaltic dykes in the Oman ophiolite: evidence from magnetic anisotropy with reference to geochemical studies. In: Peters, T.J. (Ed.), Ophiolite Genesis and the Evolution of the Oceanic Lithosphere. Kluwer, Dordrecht, pp. 55–82.

Saunders, A.D., Larsen, H.C., Fitton, J.G., 1998. Magmatic development of the Southeast Greenland margin and evolution of the Iceland plume: geochemical constraints from leg 152. In: Saunders, A.D., Larsen, H.C., Wise, S.W. (Eds.), Proc. ODP Sci. Res. 152, pp. 479–501.

Sigurdsson, H., 1987. Dyke injection in Iceland: a review. In: Halls, H.C., Fahrig, W.H. (Eds.), Mafic Dyke Swarms. Geol. Assoc. Can. Spec. Pap. 34, pp. 55–64.

Speight, J.M., Skelhorn, R.R., Sloan, T., Knapp, R.J., 1982. The dyke swarm of Scotland. In: Sutherland, D.S. (Ed.), Igneous Rocks of the British Isles. John Wiley & Sons, New York, pp. 449–459.

Staudigel, H.G., Gee, J.S., Tauxe, L., Varga, R.J., 1992. Shallow intrusive direction of sheeted dikes in the Troodos ophiolite: anisotropy of magnetic susceptibility and structural data. Geology 20, 841–844.

Tauxe, L., 1998. Paleomagnetism, Principles and Practice. Kluwer Acad, Dordrecht.

Tauxe, L., Mullender, T.A.T., Pick, T., 1996. Potbellies, wasp-waists, and superparamagnetism in magnetic hysteresis. J. Geophys. Res. 101, 571–583.

Tauxe, L., Gee, J.S., Staudigel, H., 1998. Flow direction in dikes from anisotropy of magnetic susceptibility data: the bootstrap way. J. Geophys. Res. 103, 17775–17790.

Tegner, C., Duncan, R.A., Berstein, S., Brooks, C.K., Bird, D.K., Storey, M., 1998. $^{40}Ar/^{39}Ar$ geochronology of Tertiary mafic intrusion along the east Greenland rifted margin: relation to flood basalts and the Iceland hotspot track. Earth Planet. Sci. Let. 156, 75–88.

Varga, R.J., Gee, J.S., Staudigel, H., Tauxe, L., 1998. Dykes surfaces lineations as magma flow indicators within the sheeted dyke complex of the Troodos ophiolite, Cyprus. J. Geophys. Res. 103, 5241–5256.

Walderhaug, H., 1993. Rock magnetic and magnetic fabric variations across three thin alkaline dykes from Sunnhordland, Western Norway: influence of initial mineralogy and secondary chemical alterations. Geophys. J. Int. 115, 97–108.

White, R.S., 1992. Crustal structure and magmatism of North Atlantic continental margins. J. Geol. Soc. London 149, 841–854.

White, R.S., McKenzie, D.P., 1989. Magmatism at rift zones: the generation of volcanic continental margins and flood basalts. J. Geophys. Res. 94, 7685–7729.

White, R.S., Spence, G.D., Fowler, S.R., McKenzie, D.P., Westbrook, G.K., Bowen, A.N., 1987. Magmastism at rifted continental margins. Nature 330, 439–444.